

# Fibre Wetting Processes in Wet Filtration

**Benjamin J. Mullins, Roger D. Braddock and Igor E. Agranovski**

School of Environmental Engineering, Faculty of Environmental Sciences, Griffith University, Nathan, Queensland, Australia, 4111 (E-mail: [b.mullins@mailbox.gu.edu.au](mailto:b.mullins@mailbox.gu.edu.au))

**Abstract:** The wetting behaviour of liquids on fine fibres is important in many industries, including textile manufacture and cleaning, industrial coating of fibres and wires, nanotechnology, and also in both the filtration of liquid aerosols, and wet filtration technology for industrial air pollution control. Experimental observation of the wetting processes of fibre/liquid systems (during air filtration when airflow forces are acting) shows many important features such as droplet oscillatory motion and movement or flow of droplets along fibres. The oscillation is believed to be induced by the onset of the transition from laminar to turbulent flow. Two dimensional flow in this region is usually modelled using the classical Karman vortex street, however there exist no 3D equivalents. A model incorporating the interfacial tension between the droplet and fibre and considering this as a restoring force to resist drag force, has been developed (using MATLAB) to examine this phenomenon without the need to consider the Karman vortex. The model is capable of describing the general motion of a droplet as a function of the physical parameters drag force, droplet mass, and the restoring force. A further important phenomenon noted was the effect of the fibre inclination on droplet motion down the fibre. A second model incorporating drag forces and gravitational forces acting on a droplet has been developed which allows the optimum fibre angle for maximum droplet flow to be determined for a given filter installation. This latter model is very important for filter design in wet filtration systems. Both models were compared to experimental results obtained from image analysis in the MATLAB Image Analysis Toolbox, with favourable results. Both models have the potential to improve the design/efficiency of wet filter systems, and also are relevant to other areas of fibre wetting.

**Keywords:** *Fluid Mechanics; Industrial Filtration; Fibre Wetting; Modelling*

## 1. INTRODUCTION

The relatively new process of wet filtration (for industrial air filtration), offers significant improvements over the more conventional (dry) filtration processes. Wet filtration involves coating the filter fibres with liquid or aerosol (usually water), with pollutant particles then being captured by the liquid rather than the filter. The key advantages of wet filtration over dry are significantly improved capture efficiency (especially for viscous particles or those with advanced bounce properties) and the ability of the filter to self clean (Mullins et al. 2003, Agranovski and Whitcombe 2001). Although wet filtration has been studied on a macroscopic scale, a detailed study of the fibre wetting process is needed. Some early work relating to fibre wetting (by liquid aerosols) with reference to filtration exists (Kirsch 1978). However, almost all recent work relates to non filtration applications (Carroll 1991, Bauer and Dietrich 2000). Such work does not usually consider the effects of forces such as gravity and drag, and the studies usually deal with oil droplets on horizontal fibres in water. However, Kumar and Hartland (1990) have examined droplet distortion due to gravity. The main aim of this study is to examine the liquid aerosol collection process during filtration of

aerosols on a microscopic scale, and to develop models to predict this behaviour. This process is relevant both to wet filtration, and to the capture of liquid aerosols on a dry filter. This paper will examine two important features of the wet filtration process: (1) The flow of collected liquid droplets on filter fibres, which fundamentally effects the filter self cleaning process; and (2) The airflow induced oscillation of droplets

### 1.1 Droplet Flow on Angled Fibres

Figure 1 shows a diagram of the forces inducing a droplet to flow along a fibre. Note the opposing (surface tension) force is not shown. Equation (1) has been developed, to give the drag and gravitational forces down the fibre,

$$F_Q = mg \cos(\theta_g) + 6\pi b U \mu \left[ 1 - 1.004 \left( \frac{b}{l} \right) + 0.418 \dots \right. \\ \left. \left( \frac{b}{l} \right)^3 + 0.21 \left( \frac{b}{l} \right)^4 - 0.169 \left( \frac{b}{l} \right)^5 \right]^{-1} \cos \left( \frac{\pi}{2} - \theta_g \right), \quad (1)$$

where (refer to Figure 1 for definition of  $F$  and  $\theta_g$  terms)  $l=2h-a$ ,  $a$  is the fibre radius,  $2h$  is the distance between fibre axes or the distance between the fibre axis and the edge of the channel

(only one fibre used),  $2l$  is the ‘channel’ width surrounding each fibre,  $b$  is the droplet radius (perpendicular to the fibre at the widest point),  $U$  is the face velocity, and  $\mu$  is the viscosity of the gas. The term inside the square brackets is Faxen’s correction to the Stokes’ drag, and has been applied previously to droplet on fibre cases (Kirsch 1978). Equation (1) can be simplified to:

$$F_Q = \cos(\theta_g)F_g + \cos\left(\frac{\pi}{2} - \theta_g\right)F_d. \quad (2)$$

The total surface tension force up the fibre is considered to be independent of  $\theta_g$ , although in reality there may be some small variation in tension with  $\theta_g$ . This equation can then be maximized for  $F_Q$ , to determine an angle at which the force along the fibre is maximised, thus providing the optimum self cleaning angle of the filter. This yields,

$$\theta_{MAX} = \tan^{-1}\left(\frac{F_d}{F_g}\right) + \frac{3\pi}{2}, \quad (3)$$

where  $F_Q$  is a maximum. This equation will be applied to an experimental microscopic study of the collection and flow of angled fibres in a model filter to determine the accuracy of the theory.

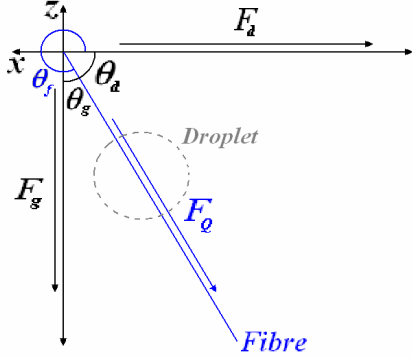


**Figure 1.** Forces acting on droplet and angles (surface tension force not included).

## 1.2 Droplet Oscillation

It has been found during experimental work detailed later that droplets oscillate on the fibre to which they are attached. This oscillation is believed to be induced by a transition of the flow field around the droplet from the laminar to the turbulent regime (this is supported by the droplet  $Re$  values – Figures 6 and 7). Flow in this region is usually modelled in 2D by the use of the Karman vortex street. However there is no 3D equivalent known analytical flow field, and another method must be devised. A model for the

droplet oscillation has thus been developed by considering the forces acting on the droplet, and considering the surface tension ( $T$ ) as a restoring force counteracting drag. Figure 2 gives a graphical representation of the terms used in the model,

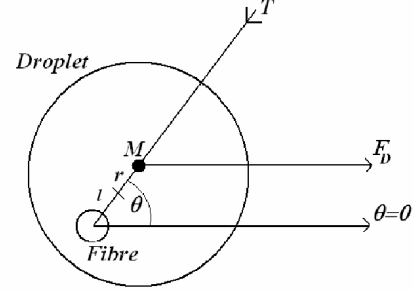


**Figure 2.** Oscillatory forces on droplet

where  $M$  is the droplet mass center,  $r$  is the displacement of  $M$  from the at rest position,  $l$  is the displacement of the rest position from  $M$ ,  $T$  is the tension (restoring force),  $F_D$  is the drag force, and  $\theta$  is the angle of the droplet relative to the airflow direction. The equations governing the droplet oscillation, can be written in radial and transverse co-ordinates, as

$$m(\ddot{r} - r\dot{\theta}^2) = -T + F_D \cos \theta, \quad (4)$$

and

$$m(r\ddot{\theta} + 2\dot{r}\dot{\theta}) = F_D \sin \theta, \quad (5)$$

where,

$$T = \begin{cases} 0 & r \leq 0 \\ \lambda(r-l) & r \geq 0 \end{cases}, \quad (6)$$

Observational evidences (see Figure 4 and Section 2.2) show the natural location of the drop down stream of the fibre ( $=l$ ). Turning on the air displaces the droplet further downstream ( $=r$ ).  $\lambda$  is a spring-like constant. These equations (4-6) can then be transformed to vector form,

$$\frac{\partial u}{\partial t} \begin{bmatrix} u_1 \\ u_2 \\ u_3 \\ u_4 \end{bmatrix} = \begin{bmatrix} u_1 u_4^2 - \frac{\lambda}{m}(u_1 - l) + \frac{F}{m} \cos(u_3) \\ 0 \\ u_4 \\ -\frac{1}{u_1}(2u_2 u_4 + F \sin(u_3)) \end{bmatrix}, \quad (7)$$

and so readily solved numerically. This model will be compared to droplet oscillation data.

## 2. METHODS – Experimental

### 2.1 Flow Experiments

To compare the theory to experimental data, an experimental cell was developed which contained 4 filter fibres, in line (usually parallel), at an angle  $\theta_f$  which was held constant during each experiment. The fibres in the cell were supplied with clean, dry air and distilled H<sub>2</sub>O aerosol from a ‘Collison’ type nebuliser – mean aerosol diameter  $2.8 \pm 0.6 \mu\text{m}$  (note in this study no pollutant aerosols were added). The flow through the cell and the mass loading of aerosol was kept constant ( $V=1.0\text{m/s}$ ). The cells were located in a polarising microscope with a x10 objective lens, and a CCD camera. Nine cell configurations were used for the experiment, each with 4 fibres, with all fibres being  $7 \pm 0.1 \mu\text{m}$  diameter glass filter fibres. Cell configurations are given in Table 1, and a cell image in Figure 3.

**Table 1.** Mean fibre angle ( $\theta_f$ ) and fibre spacing ( $S_f$ ) for each cell configuration.

$\theta_f$ – see Fig 1 (deg.)	246	258	270	283
$S_f$ ( $\mu\text{m}$ )	123	130	142	193
$\theta_f$ – see Fig 1 (deg.)	284	287	294	
$S_f$ ( $\mu\text{m}$ )	121	172	123	

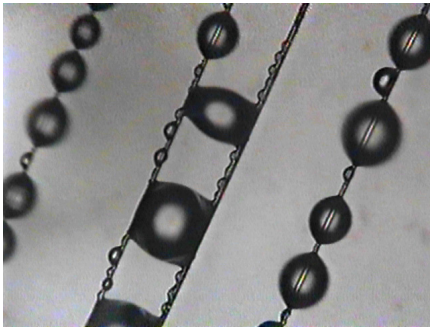


**Figure 3.** Droplets on  $7 \mu\text{m}$  glass fibre -  $V=1\text{m/s}$ ,  $\theta_f=246^\circ$ . Aerosol flow is from left to right.

For each cell, images were recorded for 8 minutes at 25fps from commencement of aerosol flow through the cell. During this time, all droplets located on the fibres were imaged, and the flow direction of the droplets were recorded. Visual examination of the real time images for each cell (8mins at 25fps) was used to determine which droplets left the fibre by flowing down. Droplets which ‘blew off’ or flowed up the fibre (not down) were not included in the analysis as they do not contribute to cleaning of the fibre. The MATLAB Image Processing Toolbox was used to

determine the cross sectional area of each droplet. The droplets were assumed to be spherical, and it is evident from Figure 3 that this is a reasonable assumption (Kirsch 1978).

### 2.2 Oscillation Experiments

A similar experimental setup and methodology was used for the oscillation experiments. However single stainless steel filter fibres



**Figure 4.** Clamshell droplets on  $28 \mu\text{m}$  SS fibre –  $V=6\text{m/s}$ , flow is left to right.

( $28 \pm 0.1 \mu\text{m}$ ) were used in the cell, and were only placed vertically (Figure 4), and the velocity and aerosol loading were varied as required to observe aerosol collection and droplet motion processes. The velocity was recorded periodically, as were the droplet images. The images were again analysed by the MATLAB Image Analysis Toolbox, to determine droplet sizes and oscillation frequencies.

## 3. METHODS – Modelling

Equation (3) is very simple and can be readily evaluated to find  $\theta_{MAX}$ . For equation (7), the MATLAB ode45 solver was used to find the solution  $u=u(t)$ . Input values for  $u$  and parameter values for  $F_D$ ,  $T$ ,  $m$  and  $r$  were obtained from the experimental results. The model used cgs units as it was found that using SI units meant that errors were magnified as many model input values were  $10^{-8}$  or smaller.

## 4. RESULTS AND DISCUSSION

### 4.1 Droplet Flow

The total volume of water flowing down the fibres in each cell (obtained from experiments) was divided by the number of fibres, the time, and the surface area of each fibre to obtain Figure 5. This approximates the droplet flow to an

equivalent film depth to allow comparison between fibre angles.

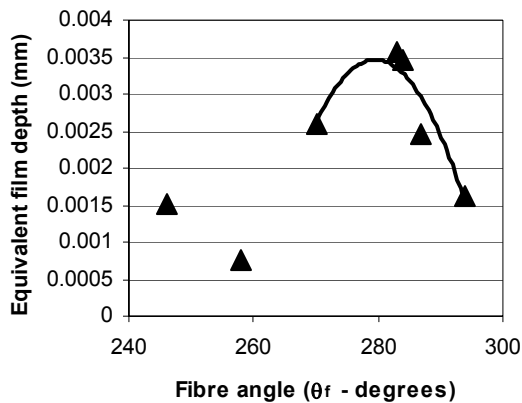


**Figure 5.** Flow depth as a function of  $\theta_f$  – parabola has been fitted to angles  $\geq 270^\circ$ .

Figures for the intersecting fibres are not shown for space reasons, as are figures detailing time between drop flow incidents/drop size. It will be noted that all cells containing fibres with  $\theta_f < 270^\circ$  had the lowest film thickness. It was noted during the experiments that for cells with all fibres where  $\theta_f \geq 270^\circ$ , the droplet flow was more even and uniform than for the cells with fibres where  $\theta_f < 270^\circ$ . Much of the flow in the latter cells was predominantly up the fibre, or the droplets simply grew in size until they blew off the fibre. Because of this, the cells with fibres  $< 270^\circ$  exhibited a significantly greater time between ‘flow’ incidents, and a significantly larger mean droplet size. The data for  $\theta_f \geq 270^\circ$  was fitted to a parabola ( $R^2=0.8726$ ), which gives a peak at  $\theta_f = 279.6^\circ$ . When the mean droplet volumes for  $\theta_f \geq 270^\circ$  are averaged and used as the droplet volume as input to the model given in equation (3), the maximum  $F_Q$  is at  $\theta_{MAX} = 277.3^\circ$ . Thus the correlation between the theory and the experimental results appears to be quite acceptable. The difference of  $2.3^\circ$  between the two could be due to the effect of differential surface tension forces (not considered), experimental error or imperfections in the parabola fit, or even imperfections in surface roughness of the fibre. It is clear that fibres where angles  $\theta_f \geq 270^\circ$  produce better fibre flow and thus better self cleaning (in the case of wet filters) than other angles. The flow is far more uniform (time between droplets) and the droplets generally smaller. Although the fibre spacings used here were much greater than those found in most filters, the results should be comparable. In the current study, some droplets were large enough to bridge 2-3 fibres (Figure 3), and these droplets

flowed just as well as smaller droplets on individual fibres, as would occur in a real filter. These results show that there is a clear optimum fibre angle for wet filters, which would optimise filter self cleaning.

## 4.2 Droplet Oscillation

Initially, a number of qualitative findings were made from observation of the experimental process. (I) the polydisperse aerosols are initially captured on the upstream face of the filter, existing as a ‘cap’ shaped droplet, the initial droplet size being determined by the size of the aerosol particle; (II) as more aerosols are captured in the same location, they coalesce into a larger cap shaped droplet; (III) eventually, the droplet grows, and reaches a point where it rotates from the upstream face of the fibre to the downstream face (approx  $180^\circ$  around the fibre), the observation being denoted as ‘R’ in Figure 6; (IV) these droplets are now larger in diameter than the fibre, so can collect aerosols which would not be collected by the fibre, and thus continue to grow by this means; (V) eventually the droplet will reach a critical size at which it begins to oscillate (around the fibre as axis - designated by ‘A’ in Figure 6).

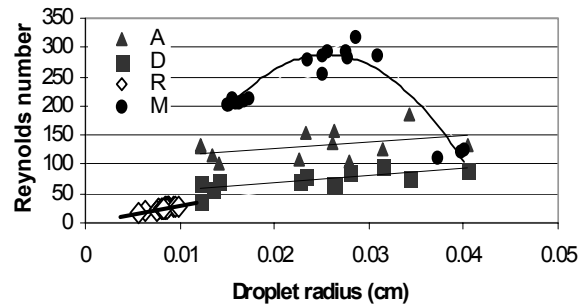


**Figure 6.** Behaviour of water droplets on  $28\mu\text{m}$  SS fibre.

Once a droplet commenced oscillation, the aerosol flow could be stopped and the flow velocity reduced, with the droplet continuing to oscillate until finally stopping at a lower velocity than which it started (‘D’ – Figure 6); (VI) The droplets would continue to grow (by capturing aerosols or coalescence) and continue to oscillate, until they left the fibre, either by being blown off or sliding down (this point denoted as ‘M’ in Figure 6). There is also some slight random motion up and down the fibre, which can bring two droplets immediately below/above each other close enough to coalesce. Uniform flow down the fibres did not occur; any flow of droplets down the fibre was erratic and intermittent. Many of these stages are observable in Figure 4, the

upstream face of the fibre is on the left hand side (LHS). The largest droplets on the fibre are oscillating, which is discernable by the comparatively fuzzy outline of these drops. Image analysis and flow measurements were used to estimate the Reynolds numbers (y axis) and droplet radii (x axis), which are shown in Figure 6. R is the point at which (III) occurs, and shows some dependence on  $Re$ . The oscillation activation (A), is clearly greater, but of similar slope to the deactivation point (D). This oscillation may be induced by the commencement of a transition of the flow regime between laminar and turbulent, which is supported by the  $Re$  values. The oscillation frequency of these droplets as a function of  $Re$  was also determined, and is given in Figure 7.

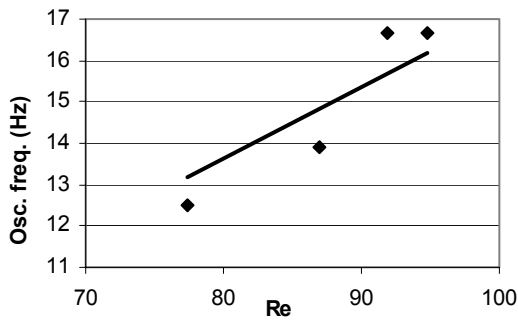


**Figure 7.** Droplet oscillation frequency

The points, M in Figure 6, show the point at which a droplet will leave the fibre (VI). The points to the left of the peak relate to the droplet being blown from the fibre by drag forces. At the peak some of the droplets begin to flow down the fibre (however this is erratic and unpredictable). The points to the right of the peak relate to all droplets flowing down the fibre. Note the curve has been fitted simply to show all points in the dataset, not to show a particular relationship – all other data has been fitted with a straight line. As velocities are reduced, the maximum stable droplet size increases, which leads to gravity becoming a more dominant force than drag and thus the droplet flows down the fibre before drag forces can break the interfacial tension holding the droplet on the fibre. It is clearly not preferable for the droplets to be blown from the fibres (as opposed to flowing down). This will not aid the self cleaning process and could lead to re-suspension of any captured contaminant aerosols. For the range of droplet sizes (radius=180-250 $\mu$ m) examined to determine oscillation rates (Figure 7), the Tension ( $T$ ) force needed to be determined, for inclusion in the model (7). For a vertical fibre ( $\theta_s=0$ ) under steady state conditions, (4) reduces to  $T=F_D$ . Measurements were taken

under these conditions and the displacement of the mass center of the drop is shown in Figure 8. Obviously the displacement is linearly related to  $T$  for the range of experimental values.

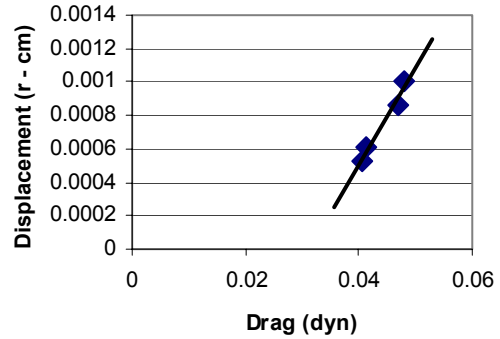


**Figure 8.** Droplet displacement due to drag

The experimental values were then inputted into the model (7), along with the initial conditions.  $F_D$  was calculated using (1). The input data were  $T=16.57r+0.03$ dyn,  $m=0.000026$ g,  $F_D=0.09$  and the initial displacement was  $r(0)=0.0006$ cm. These values correspond with an  $Re \approx 80$ , therefore from Figure 7 we would expect the model to give an oscillation frequency of 13-14Hz.. Figure 9 shows the predicted  $\theta$  value for the droplet oscillation as a function of time, while Figure 10 shows the predicted values of  $r$  as a function of time. The predicted oscillation rate of  $\approx 12$ Hz shows a good agreement between the model and the experimental data (13-14Hz).

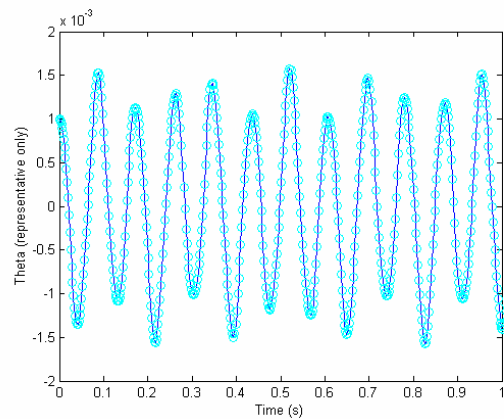


**Figure 9.** Predicted oscillation frequency of droplet ( $Re \approx 80$ ).

Note that the amplitude of the oscillation is not constant and probably arises from nonlinearities in (7). This non-uniform amplitude was supported by experimental observations, however these have not been possible to quantify at present. If the time period is extended, there seems to be a

periodic pattern to the changing amplitude. This pattern is just discernible from the 1 second timescale. The model showed some sensitivity to the initial condition on  $r(0)$ , however it would usually only vary the  $\theta(t)$  result (Figure 9) by 1Hz or so. An initial value of  $r(0)=0.75$  was chosen as producing the best results.

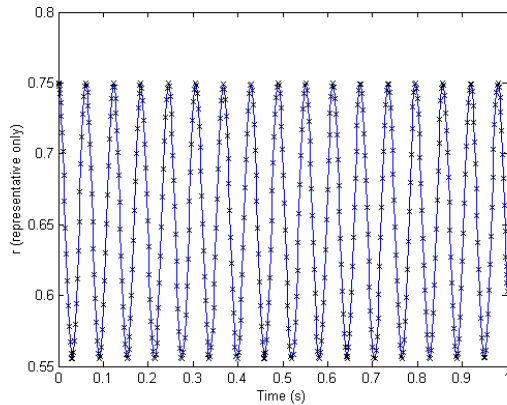


**Figure 10.** Oscillation of  $r$  over time ( $Re \approx 80$ ).

Note that (4), where  $\theta=0$ , and  $T$  is linear in  $r$ , leads to simple harmonic motion along the radial axis. The experimental data shows that this motion can occur, but it is yet to be quantified from the data. Observation indicates that the major oscillation is in the transverse or  $\theta$  direction. One question relates to the forcing of this oscillation by the air flow, arising from the transition from laminar to turbulent flow. Therefore although the droplet oscillation phenomenon is beyond current fluid mechanics analysis, this model thus far appears to be able to predict oscillation with a relatively high degree of accuracy.

## 5. FUTURE WORK

Future work will consist of: Obtaining a more accurate experimental determination for  $r$  as a function of  $F_D$ , which will improve parameter estimation for the model, sensitivity analysis of the model to input parameters and initial conditions, quantification of the variation in  $r$  and the amplitude of  $\theta$  over time in experimental results to compare with model; addition of a forcing term to the model if necessary to correct amplitude.

## 6. CONCLUSION

By determining the forces acting on a droplet on a fibre, it is possible to determine an optimum angle such that flow of droplets down the fibre will be maximized, thus optimising the self cleaning process in wet filters. The equation (4) presented in this paper can enable the optimisation of the internal filter angle for the design and manufacture of filters for wet filtration installations. If filters are manufactured with the optimum fibre orientation for the application then self cleaning will be maximised, reducing water consumption, which is an important consideration in many industries. While there remain many unknowns in droplet/fibre interactions, a better understanding of the dynamics of this phenomenon, should be able to enhance filtration theory, wet filtration designs/theory, and other areas to which fibre wetting is applicable. This should ultimately lead to an optimization of filtration regimes/flow rates for wet filter installations.

## 7. REFERENCES

- Agranovski, I. E. and J. M. Whitcombe (2001). Case Study of the Practical Use of Wettable Filters in the Removal of Sub-Micron Particles. *Chem. Eng. Tech.* **24**(5): 513-517.
- Bauer, C. and S. Dietrich (2000). Shapes, contact angles and line tensions of droplets on cylinders. *Physical Review E* **62**(2): 2428-2438.
- Carroll, B. (1991). Contact Angle, Wettability and Adhesion. *Journal of Applied Physics* **70**(493): 235.
- Kirsch, A. A. (1978). Increase in Pressure Drop in a Model Filter During Mist Filtration. *Journal of Colloid and Interface Science* **64**(1): 120 - 125.
- Kumar, A. and S. Hartland (1990). Measurement of Contact angles and Shape of a Drop on a Vertical Fiber. *Journal of Colloid and Interface Science* **136**(2): 455-469.
- Mullins, B. J., I. E. Agranovski and R. D. Braddock (2003). Particle Bounce During Filtration of Particles on Wet and Dry Filters. *Aerosol Science and Technology* **In Press**.